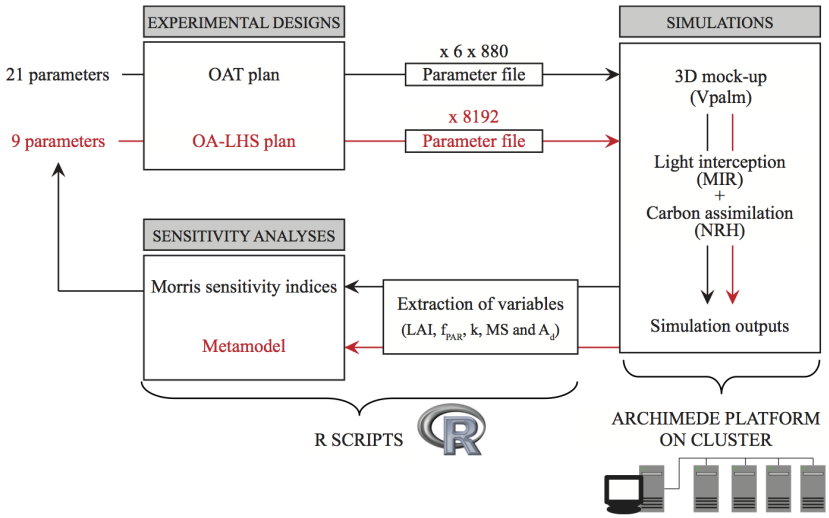

Figure S1: Schema of the overall approach with the different steps executed to perform Morris method and metamodelling (OAT: one at a time; OA-LHS: orthogonal array-based latin hypercube; MIR: light interception model ; NRH: non-rectangular hyperbola; see Table 1 for variables abbreviations).

Date	DOY	Global radiation ($MJ.m^{-2}.day^{-1}$)	Solar declination (rad)	Inverse relative distance earth-sun	Sunset hour angle (rad)	Daylight hours (h)	Daily extraterrestrial radiation ($MJ.m^{-2}.day^{-1}$)	Clearness index
2014-11-01	305	17.71	-0.27	1.02	1.59	12.11	37.63	0.47

Table S1: Climate data used for simulating photosynthesis

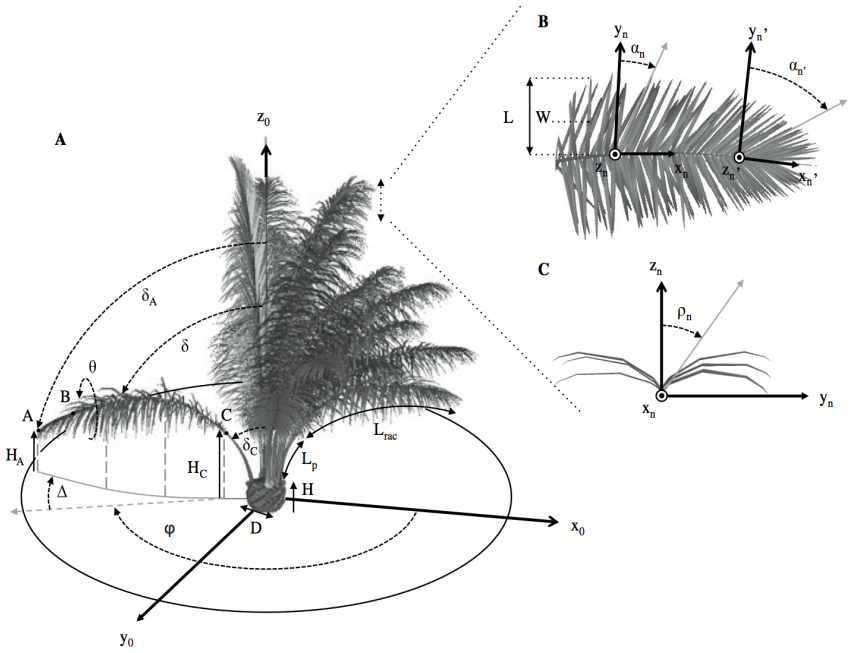

Figure S2: Geometric variables for assessing and generating 3D oil palm architecture. Point C represents the transition point between the petiole and the rachis; point B (mid-rachis) is a reference point where the cross section of the rachis becomes circular; point A is rachis tip. (**A**) Variables at the plant and leaf scale. Elevation angles (δ) are measured from the vertical reference z_C. Rachis azimuth (Δ) is measured through the projected points along the rachis on (x_C, y_C) plane. Phyllotaxis (ϕ) is measured as the azimuth angle from one leaf insertion relatively to the following one. Rachis twist (θ) is measured as the rotation angle of the rachis local plane from a vertical plane. (**B**) Detailed top view of a leaf in horizontal plane. Leaflet lengths (L) and widths (W) are measured in a sample of 10 leaflets per leaf. Axial insertion (azimuth angles α_n) is measured with reference to local rachis planes (x_n, y_n). (**C**) Detailed front view of a leaf in a transverse plane to the rachis axis. Radial insertion (elevation angle ρ_n) is measured with reference to local rachis planes (z_n, y_n). Definitions and symbols are given in Table 1.

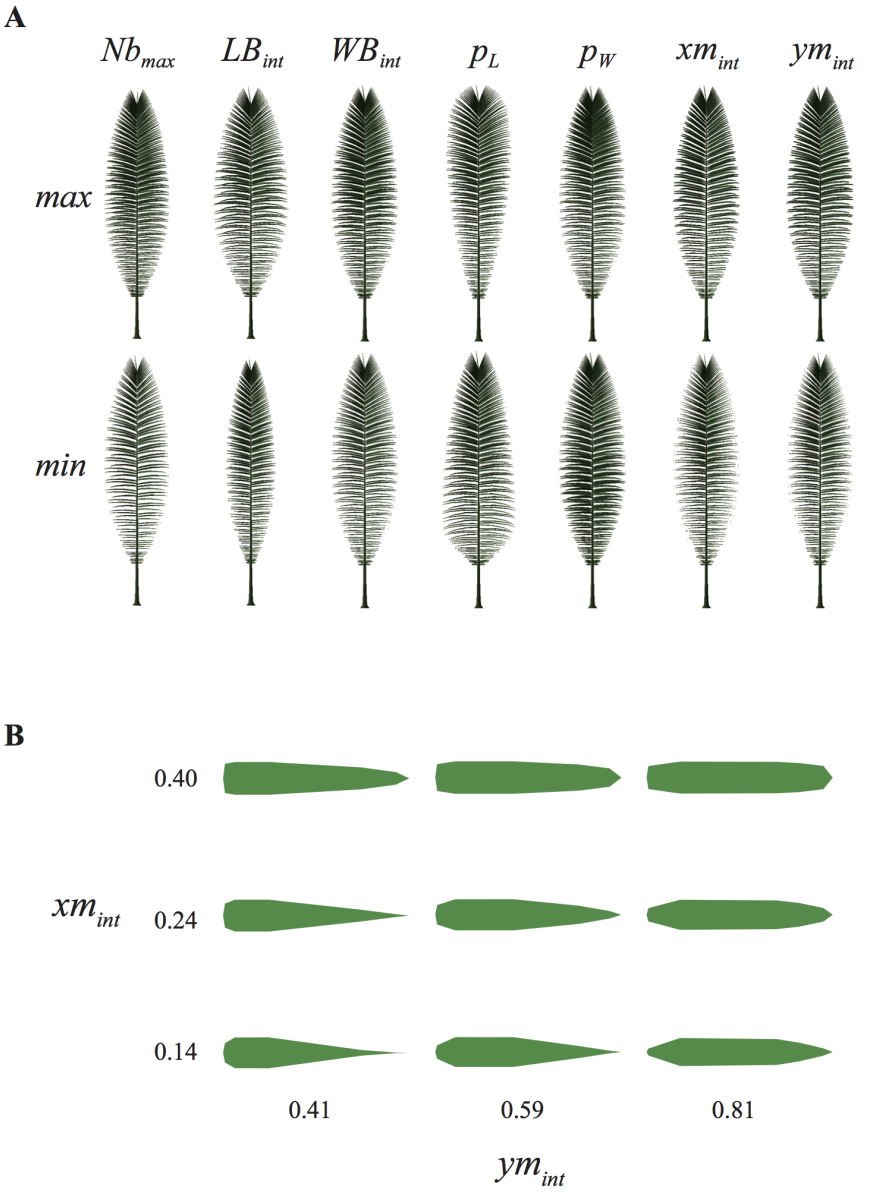

Figure S3: A) Leaf morphology depending on variation of morphometric-related parameters ($Lrac_{int}$ and $ratio_L$ being fixed to keep the same leaf length for all views). B) Leaflet morphology depending on values of the parameters xm_{int} and ym_{int}.

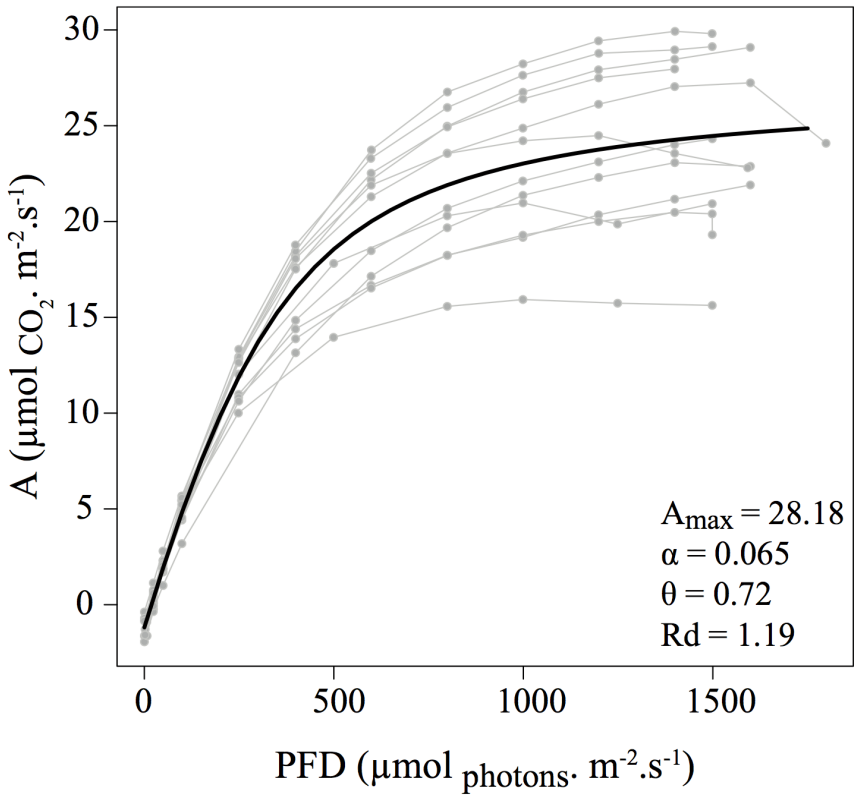

Figure S4: Calibration of non-rectangular hyperbola (NRH) curve for simulating leaf photosynthesis. Lines in grey represent the response curves obtained for 12 different oil palm leaves (from 8 individuals, on leaflet at point B from leaf rank between 9 and 17). Black line represents average model adjustment (values of calibrated parameters are presented at bottom right of the graphic).

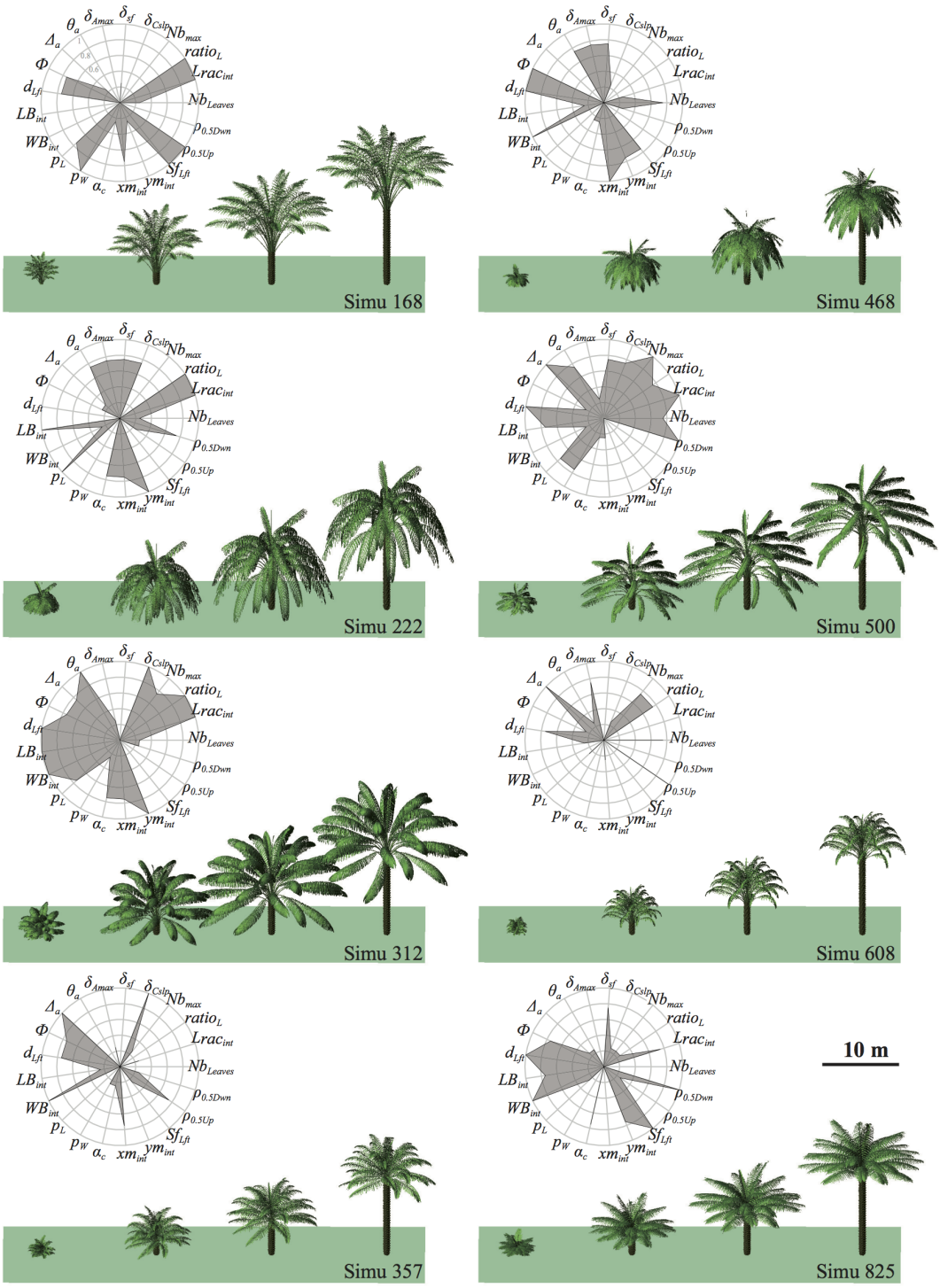

Figure S5: Examples of virtual plants generated for the Morris method, with corresponding radial plots of parameters relative value. Four developmental stages (from left to right: 50, 150, 250 and 450 leaves emerged from planting date) are represented for each simulation, all mock-ups being simulated with a similar combination of parameter (as represented in the associated radial plot).

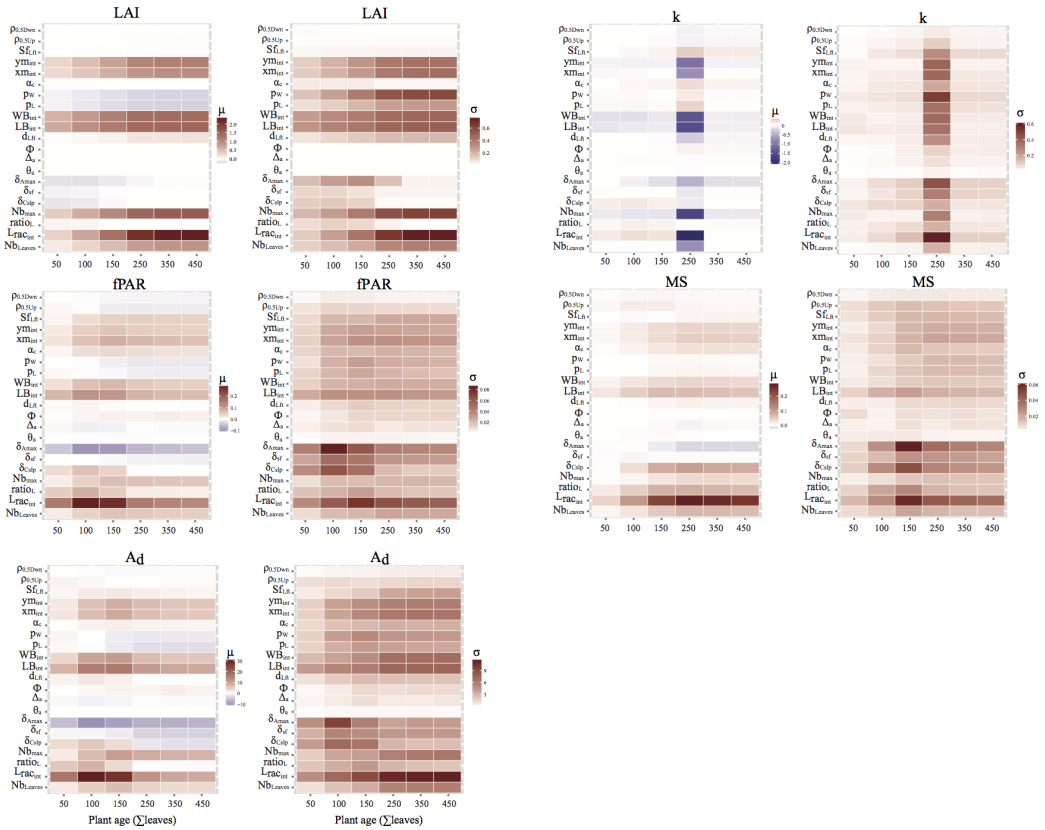

Figure S6: Heat map of elementary effects (μ) and interaction effects (σ) for LAI and the four studied outputs over plant age.

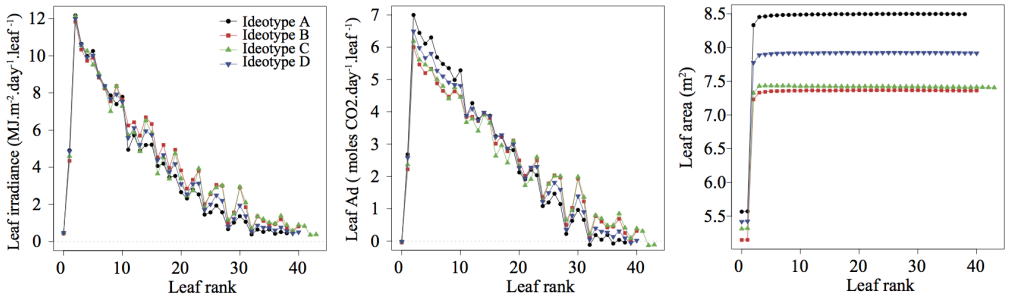

Figure S7: Daily leaf irradiance (left plot), daily assimilation (middle plot) and leaf area (right plot) for the four ideotypes.

	Estimate	Std. Error	t value	r^2(%)
(Intercept)	-561.6657	2.6638	-210.85	00.00000
$Lrac_{int}$	0.5894	0.0023	259.05	19.46048
$L_{B_{int}}$	2.1566	0.0133	162.75	36.55092
Nb_{max}	1.0274	0.0078	132.13	51.64969
$W_{B_{int}}$	34.5189	0.2277	151.61	63.60312
ym_{int}	157.0191	1.5436	101.73	70.81435
xm_{int}	303.5926	2.2966	132.19	76.66714
δ_{Amax}	-0.0849	0.0085	-10.02	81.96974
Nb_{Leaves}	7.7733	0.0897	86.66	85.07723
$Lrac_{int}$:$L_{B_{int}}$	-0.0012	0.0000	-161.84	87.45447
$Lrac_{int}$:$W_{B_{int}}$	-0.0167	0.0001	-133.03	89.20623
$Lrac^2_{int}$	-0.0001	0.0000	-123.91	90.57698
$Lrac_{int}$:Nb_{max}	-0.0004	0.0000	-113.89	91.75822
$Lrac_{int}$:Nb_{Leaves}	-0.0031	0.0000	-99.88	92.65574
ym_{int}:xm_{int}	-79.5835	0.9235	-86.18	93.33458
xm^2_{int}	-129.4009	1.6322	-79.28	93.94125
$Lrac_{int}$:xm_{int}	-0.0990	0.0012	-79.33	94.49336
$LracInt$:ym_{int}	-0.0606	0.0008	-76.92	95.04430
Nb_{max}:$W_{B_{int}}$	-0.0272	0.0004	-65.46	95.44813
$L_{B_{int}}$:Nb_{max}	-0.0015	0.0000	-62.64	95.81247
$L_{B_{int}}$:$W_{B_{int}}$	-0.0535	0.0009	-61.22	96.15116
$L^2_{B_{int}}$	-0.0032	0.0001	-54.97	96.42919
Nb^2_{max}	-0.0007	0.0000	-55.48	96.69741
$ratio_L$	32.2187	1.6662	19.34	96.95290
Nb_{max}:xm_{int}	-0.1922	0.0041	-46.69	97.15249
Nb_{max}:ym_{int}	-0.1201	0.0026	-46.16	97.35166
$W^2_{B_{int}}$	-0.7506	0.0165	-45.39	97.53281
$L_{B_{int}}$:ym_{int}	-0.2397	0.0055	-43.83	97.70474
$W_{B_{int}}$:xm_{int}	-6.1906	0.1464	-42.30	97.87080
$W_{B_{int}}$:ym_{int}	-3.9172	0.0928	-42.20	98.03650
$W_{B_{int}}$:Nb_{Leaves}	-0.1523	0.0037	-41.41	98.19554
$L_{B_{int}}$:Nb_{Leaves}	-0.0088	0.0002	-40.42	98.35124
Nb^2_{Leaves}	-0.0413	0.0010	-41.14	98.50381
$L_{B_{int}}$:xm_{int}	-0.3322	0.0087	-38.15	98.63913
Nb_{max} :Nb_{Leaves}	-0.0035	0.0001	-34.09	98.74717
ym_{int}:Nb_{Leaves}	-0.7034	0.0231	-30.50	98.83468
xm_{int}:Nb_{Leaves}	-1.0840	0.0366	-29.58	98.91355
δ^2_{Amax}	-0.0004	0.0000	-24.62	98.96878
$Lrac_{int}$:ratio	-0.0261	0.0011	-23.94	99.02276
$L_{B_{int}}$:δ_{Amax}	0.0006	0.0000	19.96	99.06008
$Lrac_{int}$:δ_{Amax}	-0.0001	0.0000	-19.40	99.09414
xm_{int}:δ_{Amax}	0.0895	0.0049	18.37	99.12492
ym^2_{int}	-11.9180	0.6542	-18.22	99.15554
Nb_{Leaves}:$ratio_L$	-0.5014	0.0320	-15.65	99.17878
$W_{B_{int}}$:δ_{Amax}	0.0074	0.0005	15.02	99.20021
ym_{int}:δ_{Amax}	0.0399	0.0031	12.92	99.21592
Nb_{max}:δ_{Amax}	0.0002	0.0000	11.97	99.22927
δ_{Amax}:Nb_{Leaves}	0.0014	0.0001	11.84	99.24199
$L_{B_{int}}$:$ratio_L$	0.0404	0.0076	5.31	99.24449
$ratio^2_L$	-6.3380	1.2590	-5.03	99.24674
ym_{int}:$ratio_L$	2.5279	0.8079	3.13	99.24755

Table S2: Summary of metamodel (*eqn* 2) adjustements to predict Ad. The order of the significant parameters results from a variance-based decomposition based on orthogonal polynomials. The estimated values of the coefficients and its standard deviation are those obtained without orthonormalization to be more easily interpretable. The fourth column (r^2) represents the cumulative multiple R-squared when all the above variables are included in the metamodel.